

Electrochemical and Spectrometric Study of GFP-AZT Interaction

Marketa Kominkova^{1,2}, Renata Kensova^{1,2}, Roman Guran^{1,2}, Ondrej Zitka^{1,2}, Jindrich Kynicky^{2,3}, Libuse Trnkova^{1,2}, Vojtech Adam^{1,2} and Rene Kizek^{1,2*}

¹ Department of Chemistry and Biochemistry, Faculty of Agronomy, Mendel University in Brno, Zemedelska 1, CZ-613 00 Brno, Czech Republic, European Union

² Central European Institute of Technology, Brno University of Technology, Technicka 3058/10, CZ-616 00 Brno, Czech Republic, European Union

³ Karel Englis College, Sujanova nam. 356/1, CZ-602 00, Brno, Czech Republic, European Union

*E-mail: kizek@sci.muni.cz

Received: 1 xxx 2014 / Accepted: 1 xxx 2014 / Published: 1 xxx 2014

In the last 18 years the highly active antiretroviral therapy (HAART) has been used for the treatment of HIV and consists of the combination of various drugs. The introduction of this type of treatment caused a significant extension of lives of patients and a reduction of side effects. However, the complete recovery of patients with HIV is still impossible. Azidothymidine (AZT) was the first drug used for the treatment of HIV and it is used in a combination with other drugs in HAART. Although the mechanism of effect of this drug is known, the mechanisms of side effects are still not sufficiently clarified. The way how to orient even in these reactions is the use of markers that allow *in vivo* monitoring of biological processes associated with the drug. As a fluorescent label the green fluorescent protein (GFP) can be used. In this study, we evaluated the link between AZT and GFP by electrochemical methods and also the change of the properties of GFP fluorescence after the binding/intercalating of AZT. We can conclude from the results obtained that the interaction between the drug and GFP takes place, but it does not adversely affect the fluorescent properties of GFP. Therefore, this protein may serve as a suitable fluorescent marker for observation of biological processes.

Keywords: Azidothymidine (AZT); zidovudine; green fluorescent protein (GFP); HIV

1. INTRODUCTION

Highly active antiretroviral therapy (HAART) was introduced in 1996 and revolutionized the existing treatment of patients infected by human immunodeficiency virus (HIV)/acquired immunodeficiency syndrome (AIDS). Currently, this type of treatment is called also as a combination antiretroviral therapy (cART) [1]. With the arrival of this therapy the incidence of opportunistic infections and premature death was significantly reduced [2]. Before the year 1996 the median of survival of young infected people was 7 years after the diagnosis, while currently it is 35 years [3]. This treatment consists of a combination of protease inhibitors (PI), nucleoside reverse transcriptase inhibitors (NRTI), and/or non-nucleoside reverse transcriptase inhibitors (NNRTI) [4].

The group of NRTI includes also azidothymidine (3'-Azido-3'-deoxythymidine, Zidovudine, AZT) and together with another drug from this class is administered as a part of HAART particularly in the treatment of HIV-1. This is the first compound that has been approved for the treatment of HIV and is still an integral part of systemic therapy [5]. AZT, as well as drugs belonging to NRTI, requires activation by phosphorylation [6], then it is followed by the end of termination and by the blocking of nucleotide-binding site for HIV-1 reverse transcriptase [7-9]. Besides this mechanism the using of this treatment also leads to the inhibition of gamma-polymerase resulting in decline in the occurrence of mtDNA [10,11]. Despite the fact that thanks to the use of AZT and other drugs under HAART the suppression of viral replication occurs in a long term, this effect is redeemed by a number of side effects, which follow exactly the decrease of the mtDNA and thus lead to mitochondrial toxicity that leads to a liver failure and a lactic acidosis [10]. Side effects associated with HAART therapy include anaemia, cardiomyopathy, gastrointestinal disturbance, drug-induced hypersensitivity, nephrotoxicity, pancreatitis, ototoxicity and others [6]. AZT, compared to other drugs from NRTI group, shows markedly less inhibition of gamma-polymerase, but through other mechanisms associated with this has similar side effects [12].

Despite considerable research efforts related to a HIV treatment there are not known all the mechanisms of action of these drugs. The possibility of *in vivo* imaging of drug interaction in an organism can help to elucidate these mechanisms [13]. For the labelling of target molecules green fluorescent protein (GFP), which thanks to its fluorescent properties allows *in vivo* monitoring of events in a real-time, can be used [14]. The aim of this study was to assess the bond between AZT and GFP electrochemically, and further analysis of the GFP fluorescent properties influenced by the binding of AZT.

2. EXPERIMENTAL PART

2.1. Chemicals and pH measurement

Azidothymidine, thymine, water and other chemicals listed in the text were purchased from Sigma-Aldrich (St. Louis, MO, USA) meet the specification of American Chemical Society (ACS), unless stated otherwise. The deionised water was prepared using reverse osmosis equipment Aqual 25 (Aqual s.r.o., Brno, Czech Republic). The deionised water was further purified by using apparatus Milli-Q Direct QUV equipped with an UV lamp from Millipore (Billerica, MA, USA). The resistance was 18 M Ω . The pH was measured using pH meter WTW inoLab (Weilheim, Germany).

2.2. Preparation of GFP - Chemical Transformation

The plasmid pGLO (Bio-Rad, CA, USA) contained the gene forming Green Fluorescent Protein (GFP), which comes from bioluminescent jellyfish, *Aequorea victoria*. GFP is under the control of the arabinose-induced promoter araBAD and the araC gene encoding a regulator protein that turns the GFP gene on and off. The chemical transformation protocol was performed following the instructions of Invitrogen Competent cells using as a host the TOP10 Chemically Competent *E. coli* strain (Invitrogen Corporation, CA, USA). Bacteria transformed with pGLO plasmid were selected by ampicillin resistance. The positive transformants were confirmed by PCR and In Vivo Fluorescence Imaging.

2.3. Preparation of GFP - Growth Conditions and Isolation of Soluble Protein Fraction

The positive transformants were grown in LB (Luria-Bertani) broth with 100 mg.L⁻¹ ampicillin and 0.2% arabinose shaking at 32 °C overnight. Bright green cells were harvested by centrifugation at 4000 rpm for 10 min. The pellet was resuspended thoroughly by rapidly pipetting up and down several times in TE buffer (1 mM EDTA pH 8, 10 mM TRIS-HCl pH 8). To initiate enzymatic digestion of the bacterial cell wall the 10 mg.mL⁻¹ of fresh lysozyme (Sigma-Aldrich) was added and then the resuspended bacterial pellet was frozen. The protein fraction was harvested by centrifugation for 10 min at 14000 rpm at 4 °C.

GFP was purified from the bacterial lysate using hydrophobic interaction chromatography (HIC) columns (Macro-Prep® Methyl HIC Column; Bio-Rad, CA, USA). The protein elution was made with TE buffer.

2.4. Preparation of samples

The following samples were prepared for all measurements: thymine for FIA-ED in concentration of 100 µg.mL⁻¹; AZT in concentrations of 3, 6, 13, 25, 50 and 100 µg.mL⁻¹; GFP in same concentrations as AZT; AZT-GFP with ratios of 3:100, 6:100, 13:100, 25:100, 50:100 and 100:100; GFP-AZT in same ratios as before. Samples were incubated at 25 °C for 30 minutes before measurements. All samples were prepared in ACS water.

2.5. Gel electrophoresis of GFP and its fluorescence detection

Sample of GFP was mixed with protein loading buffer (PLB) (under reducing conditions PLB with mercaptoethanol) in a ratio of 1:1 and placed in the wells of the 12.5% polyacrylamide gel (w/w) prepared from 30% acrylamide/bis-acrylamide solution (37.5:1). Electrophoresis ran in 1× tris-glycine-SDS running buffer (3.02 g of Tris, 14.4 g of glycine, 1 g of SDS, ddH₂O to a final volume of 1 L) for 90 min at a voltage of 120 V in the electrophoretic bath (Bio-Rad, CA, USA). Fluorescence of GFP in gel was measured by In-vivo Xtreme (Carestream, CT, USA) using excitation at 410 nm and emission at 535 nm.

2.6. Fluorescence study of GFP

Fluorescence was measured by multifunctional microplate reader Tecan Infinite M200 PRO (TECAN, Switzerland). As an excitation wavelength 410 nm was used and the fluorescence scan was measured within the range from 450 to 750 nm. The detector gain was set to 100. Both tested sets were placed in UV-transparent 96 well microplate with flat bottom (CoStar; Corning, NY, USA). To each well 100 μL of sample was pipetted. All measurements were performed at 30 °C controlled by Tecan Infinite M200 PRO (TECAN, Switzerland).

2.7. Determination of total protein concentration

Total protein concentration was determined by BS-400 automated spectrophotometer (Mindray, China) using pyrogallol red (SKALAB Svitavy, CZ). The pyrogallol red protein assay is based upon formation of a blue protein-dye complex in the presence of molybdate under acidic conditions (pH 2.5). 150 μL volume of reagent mixture (1:1) R1:R2 (50 mM succinic acid, 3.47 mM sodium benzoate, 0.06 mM sodium molybdate, 1.05 mM sodium oxalate and 0.07 mM pyrogallol red) is pipetted into a plastic cuvette with subsequent addition of 8 μL of a sample. Absorbance is measured at 605 nm after 10 minutes of incubation. Resulting value is calculated from the absorbance value of the pure reagent mixture and from the absorbance value after 10 minutes of incubation with the sample.

2.8. Electrochemical study of AZT

Determination of AZT-GFP complex by square wave voltammetry was performed with 797 VA Computrace instrument connected to 889 IC Sample Center (Metrohm, Switzerland), using a standard cell with three electrodes. A hanging mercury drop electrode (HMDE) with a drop area of 0.4 mm² was the working electrode. An Ag/AgCl/3M KCl electrode was the reference and platinum electrode was the auxiliary one. The analysed samples were deoxygenated prior to measurements by purging with argon (99.999 %). Phosphate buffer (0.085 M Na₂HPO₄ and 0.075 M NaH₂PO₄, pH adjusted to 8.0) was used as a supporting electrolyte. The supporting electrolyte was exchanged after each analysis. The parameters of the measurement were as follows: initial potential -0.1 V, end potential -1.7 V, deoxygenating with argon 120 s, time accumulation 120 s, voltage step 6 mV, modulation amplitude 0.02 V, deposition potential -0.1 V, frequency 280 Hz (sweep rate 1.6663 V.s⁻¹), volume of injected sample 20 μL (10 μL of AZT and 10 μL of GFP), volume of measurement cell 2 mL (20 μL of the sample and 1980 μL of the phosphate buffer).

2.9. Electrochemical study of GFP

Measurements were done in Brdicka buffer by differential pulse voltammetry with following equipment: 747 VA Stand instrument connected to 693 VA Processor and 695 Autosampler (Metrohm, Switzerland), using a standard cell with three electrodes, cooled sample holder and measurement cell to 4 °C by Julabo F25 (JULABO, Germany). A hanging mercury drop electrode (HMDE) with a drop area of 0.4 mm² was the working electrode. An Ag/AgCl/3M KCl electrode was the reference and platinum electrode was auxiliary. For data processing VA Database 2.2 by Metrohm CH was

employed. The analysed samples were deoxygenated prior to measurements by purging with argon (99.999 %) saturated with water for 120 s. Brdicka electrolyte (1 mM $\text{Co}(\text{NH}_3)_6\text{Cl}_3$ and 1 M ammonia buffer ($\text{NH}_3(\text{aq})$ and NH_4Cl , pH = 9.6) was used. The supporting electrolyte was exchanged after each analysis. The parameters of the measurement were as follows: initial potential -0.7 V, end potential -1.75 V, modulation time 0.057 s, time interval 0.2 s, step potential 2 mV, modulation amplitude -250 mV, $E_{\text{ads}} = 0$ V, volume of sample 20 μL (10 μL GFP and 10 μL AZT), volume of measurement cell 2 mL (20 μL of sample and 1980 μL Brdicka electrolyte). The tip dropped 10 μL GFP and 10 μL AZT to the measured cell, added Brdicka electrolyte and this mixture was kept interacting for 30 min. After that the solution was measured.

2.10. Flow injection analysis with electrochemical detection

Flow injection analysis (FIA) system consisted of a chromatographic pump Model 584 ESA (ESA Inc., MA, USA) with working range $0.001\text{-}9.999\text{ mL}\cdot\text{min}^{-1}$ and of electrochemical detector CoulArray (ESA Inc., MA, USA). The electrochemical detector included one flow cell (Model 6210; ESA Inc., MA, USA). The cell consisted of four working carbon porous electrodes, each one with auxiliary and dry Pd/ H_2 reference electrodes. Both the detector and the reaction coil/column were thermostated. The 20 μL of sample was injected automatically by autosampler (Model 542; ESA Inc., MA, USA). During the analysis the samples were stored in the carousel. Mobile phase consisted of phosphate buffer (pH 7.5, 20 mM). Flow rate of a mobile phase was $1\text{ mL}\cdot\text{min}^{-1}$.

2.11. Descriptive statistics

Data were processed using MICROSOFT EXCEL® (Microsoft, WA, USA). Results were expressed as mean \pm standard deviation (S.D.) unless noted otherwise (EXCEL®). Differences with $p < 0.05$ were considered significant and were determined by using of one way ANOVA test (particularly Scheffe test), which was applied for means comparison.

3. RESULTS AND DISCUSSION

AZT belongs to nucleoside reverse transcriptase inhibitors (NRTI) and is structurally related to the endogenous nucleoside thymidine with an azido group in place of the hydroxyl group at the 3' position of the deoxyribose ring. Prior to be activated it has to be phosphorylated, subsequently it is engaged in a process of reverse transcription of viral RNA [15]. The scheme of action mechanism of AZT in HIV replication cycle is shown in Figs. 1A and 1B.

Although AZT belongs to the most effective drugs for treatment of HIV, it has a variety of side effects [6]. For monitoring drug effects at the cellular level the fluorescent labelling with a green fluorescent protein (GFP) can be used [14]. The most probably interaction of AZT with GFP is shown in Fig. 1C. The interaction between GFP and AZT was evaluated by fluorescence spectroscopy, square wave voltammetry (SWV), differential pulse voltammetry (DPV) Brdicka reaction and FIA-ED.

Before the characterization of GFP-AZT interaction, the absorption and fluorescence spectra were measured (Figs. 2A and 2B) and the SDS-PAGE of GFP with fluorescence visualization was made too (Fig. 2C). The fluorescence spectra of AZT (data not shown) demonstrated fluorescence on the level of blank. The maximal fluorescence of GFP was detected app. 512 nm.

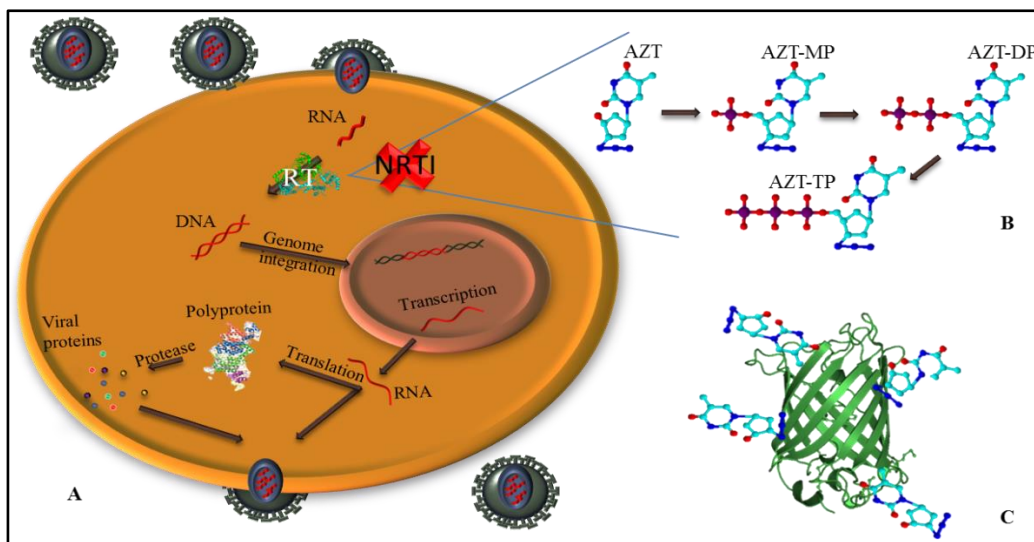


Figure 1. (A) HIV replication cycle - HIV virus, which enters the cell, releases its RNA and reverse transcriptase (RT), which enables the transcription of RNA to DNA that is also integrated into the genome in the nucleus where transcription occurs. This newly formed RNA leaves the nucleus. Part of the RNA is used as a template for translation of the polyprotein that is cleaved by proteases on the viral proteins, which are fold with RNA in the virion that leaves the infected cell. (B) The mechanism of action of a nucleoside reverse transcriptase inhibitor (NRTI) - Azidothymidine (AZT). Before the effect of drug, AZT must be activated through the three-step intracellular kinases phosphorylation, first to monophosphate (AZT-MP), further to diphosphate (AZT-DP) and to the triphosphate (AZT-TP). AZT-TP inhibits the activity of reverse transcriptase by competing with its natural nucleotide counterpart thymidine triphosphate for incorporation into newly synthesized viral DNA. Once incorporated, it leads to DNA chain termination and stops further DNA synthesis. (C) Scheme of the green fluorescent protein (GFP) with bound molecules of AZT.

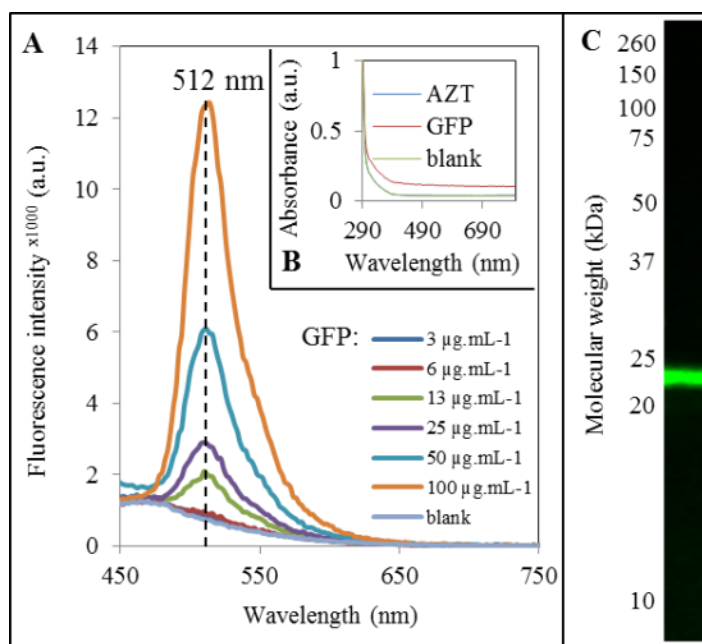


Figure 2. (A) Fluorescence spectra of GFP in different concentrations and of blank; the fluorescence of AZT was practically same as of blank and therefore it isn't shown. (B) Absorption spectra of AZT ($100 \mu\text{g.mL}^{-1}$), GFP ($100 \mu\text{g.mL}^{-1}$) and blank. The blue curve of AZT is overlapped by

the green curve of blank. All samples were measured by Tecan Infinite M200 Pro. Absorption scan was measured within the range from 290 to 800 nm. Fluorescence scan was measured with an excitation wavelength 410 nm and emission from 450 nm to 750 nm. The volume of measured samples in the microplate wells was 100 μL . Measurements were performed at 30 $^{\circ}\text{C}$. (C) Fluorescence of GFP in gel detected by In-vivo Xtreme. Excitation at 410 nm and emission at 480-535 nm.

3.1. Fluorescence measurement

The dependence of maximal fluorescence intensity (a.u.) on the concentration of GFP ($\mu\text{g}\cdot\text{mL}^{-1}$) is shown in Fig. 3A. It is a comparison of maximal fluorescence of GFP in concentrations of 3, 6, 13, 25, 50 a 100 $\mu\text{g}\cdot\text{mL}^{-1}$ with maximal fluorescence of GFP in same concentrations after the addition of AZT in final constant concentration of 100 $\mu\text{g}\cdot\text{mL}^{-1}$. The dependence of maximal fluorescence intensity (a.u.) of constant amount of GFP (100 $\mu\text{g}\cdot\text{mL}^{-1}$) with addition of AZT in final concentrations of 3, 6, 13, 25, 50 and 100 $\mu\text{g}\cdot\text{mL}^{-1}$ is shown in Fig. 3B. It was found that the fluorescence of GFP wasn't significantly influenced (at the significance level $\alpha = 0.05$) due to addition of AZT, which could be useful for detection of GFP-AZT complex and for its tracking. From determination of total protein concentrations in AZT, AZT-GFP and GFP samples (Fig. 3C) was found that with higher added concentrations of AZT to constant amount of GFP (100 $\mu\text{g}\cdot\text{mL}^{-1}$) the lower total protein concentrations were detected. It is probably caused by the interaction of AZT with GFP, which could result in worse formation of blue protein complex, by which absorbance for protein determination is measured.

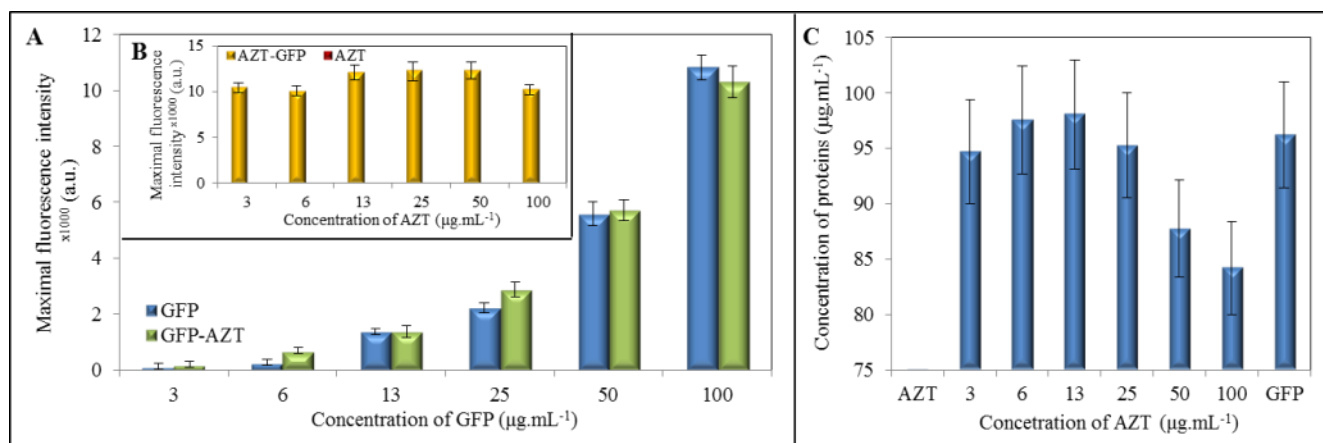


Figure 3. The fluorescence detection of GFP influenced by the addition of AZT and determination of total protein concentration. (A) Constant addition of AZT (100 $\mu\text{g}\cdot\text{mL}^{-1}$) to the increasing concentrations of GFP in comparison with control samples of GFP without AZT addition. (B) The influence of addition of AZT in increasing concentrations to the constant concentration of GFP (100 $\mu\text{g}\cdot\text{mL}^{-1}$) in comparison with control samples of AZT without GFP addition. All samples were measured by Tecan Infinite M200 Pro. Absorption scan was measured within the range from 290 to 800 nm. Fluorescence scan was measured with an excitation wavelength 410 nm and emission from 450 nm to 750 nm. The volume of measured samples in the microplate wells was 100 μL . Measurements were performed at 30 $^{\circ}\text{C}$. (C) Determination of total concentration of proteins in AZT sample (100 $\mu\text{g}\cdot\text{mL}^{-1}$), in samples with constant amount of GFP (100 $\mu\text{g}\cdot\text{mL}^{-1}$) with addition of AZT in increasing concentrations (shown in figure) and in GFP sample (100 $\mu\text{g}\cdot\text{mL}^{-1}$). Measurements were performed on BS-400 (Mindray, China) using pyrogallol red. The absorbance of blue protein complex was measured at 605 nm.

3.2. Electrochemical measurement

Differential pulse voltammograms of GFP in different concentrations measured in Brdicka solution are shown in Fig. 4A and square wave voltammograms of AZT in different concentrations measured in phosphate buffer (pH 8.0) are shown in Fig. 4B. The dependence of peak height of GFP (nA) on the concentration of GFP ($\mu\text{g.mL}^{-1}$) is shown in Fig. 4C. It is a comparison of electrochemical detection of GFP in concentrations of 3, 6, 13, 25, 50 and 100 $\mu\text{g.mL}^{-1}$ with electrochemical detection of GFP in same concentrations after the addition of AZT in final constant concentration of 100 $\mu\text{g.mL}^{-1}$. It clearly follows from the results obtained that with constant addition of AZT to different concentrations of GFP the peak heights of GFP always decreased probably due to interaction between GFP and AZT. The dependence of peak height of AZT (nA) on the concentration of AZT ($\mu\text{g.mL}^{-1}$) is shown in Fig. 4D. It is a comparison of electrochemical detection of AZT in concentrations of 3, 6, 13, 25, 50 and 100 $\mu\text{g.mL}^{-1}$ with electrochemical detection of AZT in same concentrations after the addition of GFP in final constant concentration of 100 $\mu\text{g.mL}^{-1}$.

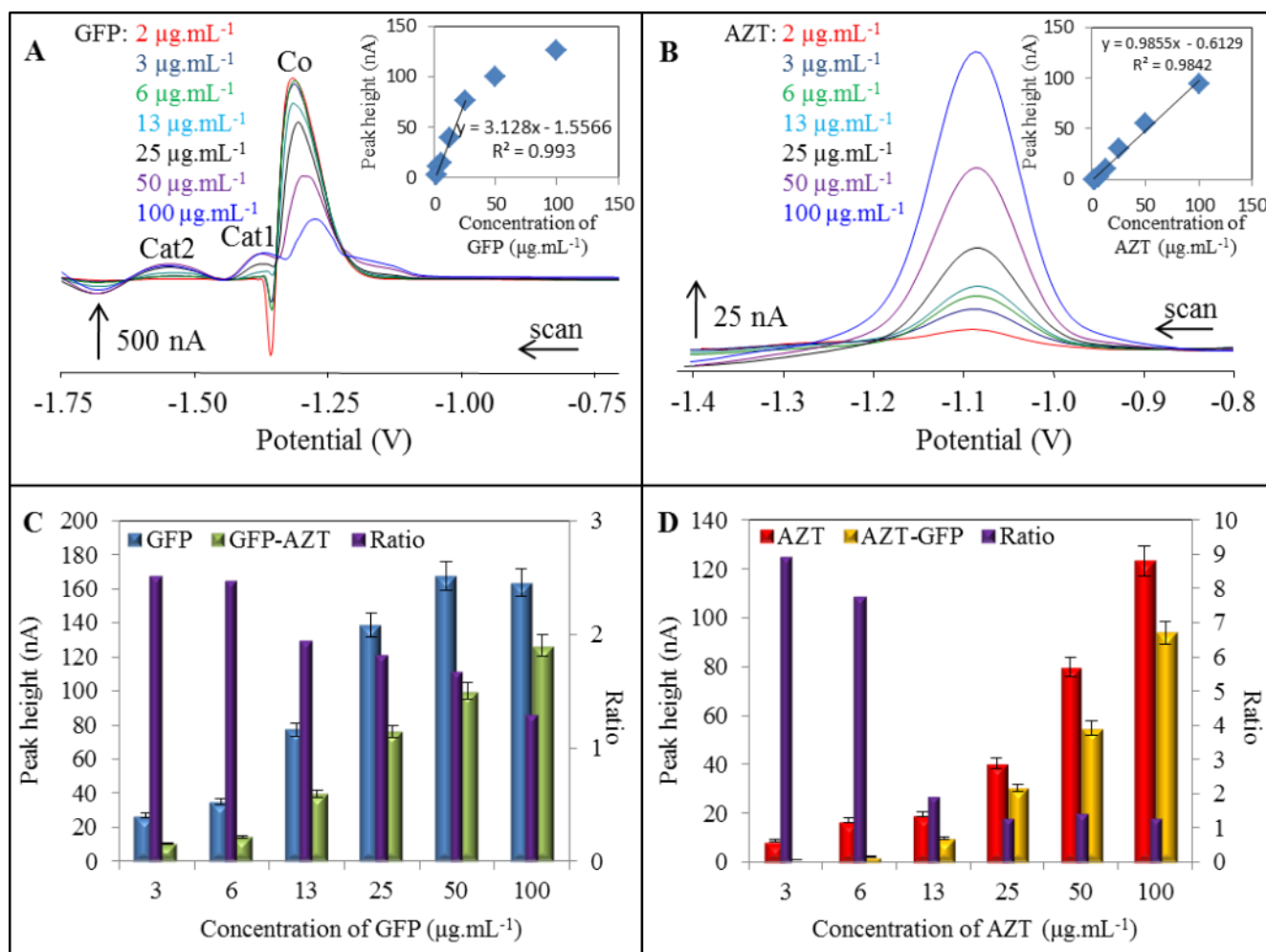


Figure 4. The electrochemical detection of GFP influenced by the addition of AZT. (A) Differential pulse voltammograms of GFP measured in Brdicka solution. Signal of GFP is expressed as Cat2 peak. Calibration curve is shown in inset. (B) Square wave voltammograms of AZT. Calibration curve is shown in inset. (C) Constant addition of AZT (100 $\mu\text{g.mL}^{-1}$) to the increasing concentrations of GFP in comparison with control samples of GFP without AZT addition. (D) The influence of addition of AZT in increasing concentrations to the constant

concentration of GFP ($100 \mu\text{g.mL}^{-1}$) in comparison with control samples of AZT without GFP addition. In figures C and D there are also expressed the ratios (purple colour) of GFP to GFP-AZT and of AZT to AZT-GFP.

These results show that after the constant addition of GFP to different concentrations of AZT the peak heights of AZT always decreased. The ratio of reported detected concentration by both electrochemical methods GFP-AZT (by Brdicka's method) and AZT-GFP (by SWV method) show that the formation of GFP-AZT complex occurred and that the highest degree of interaction represented by highest ratio value, which was detected in lower concentrations of studied substances by both methods. The electrochemical detection of AZT in the presence of biomolecules like proteins isn't influenced by their presence as was previously shown in [16]. Even the suitability of Brdicka's reaction method was successfully confirmed in a study of structural change of proteins making complex on the surface of mercury electrode [17]. Other uses of Brdicka's reaction for detection of proteins were mentioned in [18,19]. The interactions of protein with some chemicals can be studied also by SWV as it was mentioned in the study of metallothionein interacting with chicken polyclonal antibodies [20]. Therefore, we assumed the obtained results probably described the interaction between GFP and AZT.

3.3. Electrochemical measurement

As an additional electrochemical approach previously verified for study of complex creation between peptide and drug [21] we attempted to use the FIA-ED methods employing the glassy carbon electrode to evaluate the interaction between protein and drug.

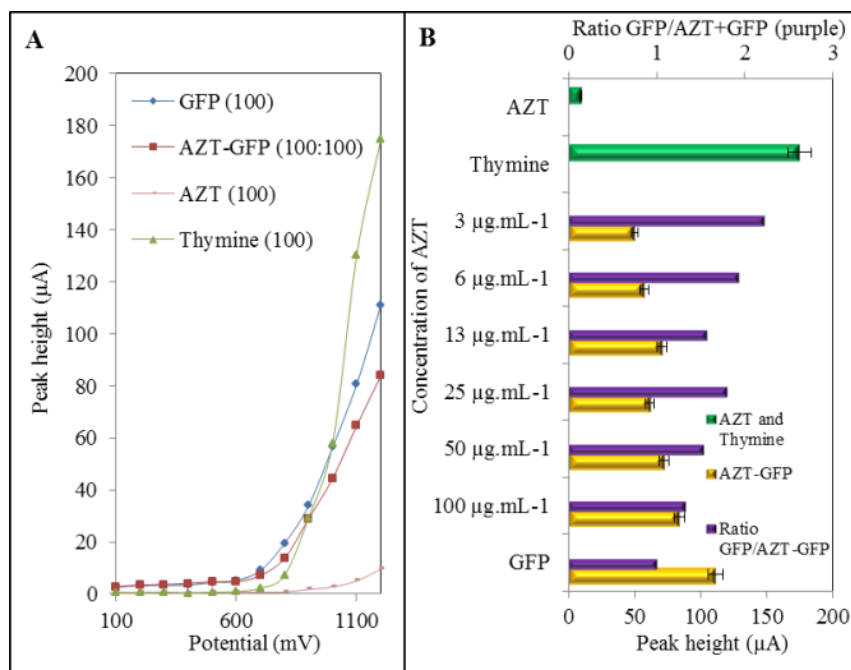


Figure 5. (A) HDVs for thymine ($100 \mu\text{g.mL}^{-1}$), AZT ($100 \mu\text{g.mL}^{-1}$), GFP ($100 \mu\text{g.mL}^{-1}$) and for AZT-GFP complex ($100:100$). (B) The expression of signal changes at the potential 1200 mV, when the highest peak heights were detected. The concentrations of AZT added to the constant amount of GFP ($100 \mu\text{g.mL}^{-1}$) were 3, 6, 13, 25, 50 and $100 \mu\text{g.mL}^{-1}$. The ratio of GFP (100

$\mu\text{g.mL}^{-1}$) to AZT-GFP is also shown (purple colour). Other experimental details see in chapters 2.4. and 2.10.

The HDVs from FIA-ED analysis of thymine ($100 \mu\text{g.mL}^{-1}$), AZT ($100 \mu\text{g.mL}^{-1}$), GFP ($100 \mu\text{g.mL}^{-1}$) and AZT-GFP complex (100:100) are shown in Fig. 5A. In Fig. 5B there are also shown the highest peak heights, measured at 1200 mV potential, of GFP ($100 \mu\text{g.mL}^{-1}$) with additions of AZT in concentrations of 3, 6, 13, 25, 50 and $100 \mu\text{g.mL}^{-1}$. The ratio of GFP ($100 \mu\text{g.mL}^{-1}$) to AZT-GFP complex with various concentrations of added AZT is also shown in this figure. These results show that with higher added concentration of AZT to the constant amount of GFP the peak height was amazingly higher. It is probably due to forming of thymine during electrochemical reaction. Thymine has similar response and can thus contribute to the overall signal height at 1200 mV. Nevertheless, the highest signal was observed with GFP only ($100 \mu\text{g.mL}^{-1}$). The ratio shows that the highest degree of interaction was detected in lower concentrations of added AZT to GFP and it corresponds with the results obtained with previous electrochemical methods (Figure 4).

4. CONCLUSIONS

The aim of our study was the confirmation of GFP-AZT complex formation and its characterization by DPV, SWV, FIA-ED and fluorescence spectroscopy. From the DPV of GFP/GFP-AZT in Brdicka reaction and from the SWV of AZT/AZT-GFP we found that the complex of GFP-AZT was formed and that the highest degree of interaction was observed in lower concentrations of added AZT (GFP) to the constant amount of GFP (AZT). Similar results were obtained by FIA-ED. We also found that AZT bound to GFP doesn't significantly influence the fluorescence of GFP and thus the GFP could be used as a suitable fluorescent label of AZT.

ACKNOWLEDGEMENTS

Financial support from NanoBioMetalNet CZ.1.07/2.4.00/31.0023 is highly acknowledged. We would like to thank to Iva Blazkova, Hana Buchtelova, Libor Janu, Monika Kremplova, Petr Michalek, Amitava Moulick, Pavlina Sobrova, Martina Stankova and Jan Zitka for their excellent assistance.

References

1. S. M. Hammer, M. S. Saag, M. Schechter, J. S. G. Montaner, R. T. Schooley, D. M. Jacobsen, M. A. Thompson, C. C. J. Carpenter, M. A. Fischl, B. G. Gazzard, J. M. Gatell, M. S. Hirsch, D. A. Katzenstein, D. D. Richman, S. Vella, P. G. Yeni and P. A. Volberding, *JAMA-J. Am. Med. Assoc.*, 296 (2006) 827.
2. V. Leung, J. Gillis, J. Raboud, C. Cooper, R. S. Hogg, M. R. Loutfy, N. Machouf, J. S. G. Montaner, S. B. Rourke, C. Tsoukas, M. B. Klein and C. Collaboration, *Plos One*, 8 (2013) 1.
3. N. Lohse, A. B. E. Hansen, G. Pedersen, G. Kronborg, J. Gerstoft, H. T. Sorensen, M. Vaeth and N. Obel, *Ann. Intern. Med.*, 146 (2007) 87.
4. M. G. Sension, *J. Assoc. Nurses Aids Care*, 18 (2007) S2.
5. A. Khandazhinskaya, E. Matyugina and E. Shirokova, *Expert Opin. Drug Metab. Toxicol.*, 6 (2010) 701.
6. T. N. Kakuda, *Clin. Ther.*, 22 (2000) 685.

7. M. Guerard, J. Koenig, M. Festag, S. D. Dertinger, T. Singer, G. Schmitt and A. Zeller, *Toxicol. Sci.*, 135 (2013) 309.
8. L. Hansen, I. Parker, L. M. Roberts, R. L. Sutliff, M. O. Platt and R. L. Gleason, *J. Biomech.*, 46 (2013) 1540.
9. O. A. Olivero, *Environ. Mol. Mutagen.*, 48 (2007) 215.
10. W. Lewis, B. J. Day and W. C. Copeland, *Nat. Rev. Drug Discov.*, 2 (2003) 812.
11. M. D. Lynx and E. E. McKee, *Biochem. Pharmacol.*, 72 (2006) 239.
12. E. E. McKee, A. T. Bentley, M. Hatch, J. Gingerich and D. Susan-Resiga, *Cardiovasc. Toxicol.*, 4 (2004) 155.
13. P. Auewarakul, V. Paungcharoen, S. Louisirirochanakul and C. Wasi, *Asian Pac. J. Allergy Immunol.*, 19 (2001) 139.
14. N. Hayes, E. Howard-Cofield and W. Gullick, *Cancer Lett.*, 206 (2004) 129.
15. X. Y. Tu, K. Das, Q. W. Han, J. D. Bauman, A. D. Clark, X. R. Hou, Y. V. Frenkel, B. L. Gaffney, R. A. Jones, P. L. Boyer, S. H. Hughes, S. G. Sarafianos and E. Arnold, *Nat. Struct. Mol. Biol.*, 17 (2010) 1202.
16. J. Vacek, Z. Andryšik, L. Trnkova and R. Kizek, *Electroanalysis*, 16 (2004) 224.
17. O. Zitka, S. Krizkova, D. Huska, V. Adam, J. Hubalek, T. Eckschlager and R. Kizek, *Electrophoresis*, 32 (2011) 857.
18. S. Skalickova, O. Zitka, L. Nejd, S. Krizkova, J. Sochor, L. Janu, M. Ryvolova, D. Hynek, J. Zidkova, V. Zidek, V. Adam and R. Kizek, *Chromatographia*, 76 (2013) 345.
19. P. Sobrova, L. Vyslouzilova, O. Stepankova, M. Ryvolova, J. Anyz, L. Trnkova, V. Adam, J. Hubalek and R. Kizek, *Plos One*, 7 (2012) 1.
20. L. Trnkova, S. Krizkova, V. Adam, J. Hubalek and R. Kizek, *Biosens. Bioelectron.*, 26 (2011) 2201.
21. O. Zitka, D. Huska, S. Krizkova, V. Adam, G. J. Chavis, L. Trnkova, A. Horna, J. Hubalek and R. Kizek, *Sensors*, 7 (2007) 1256.